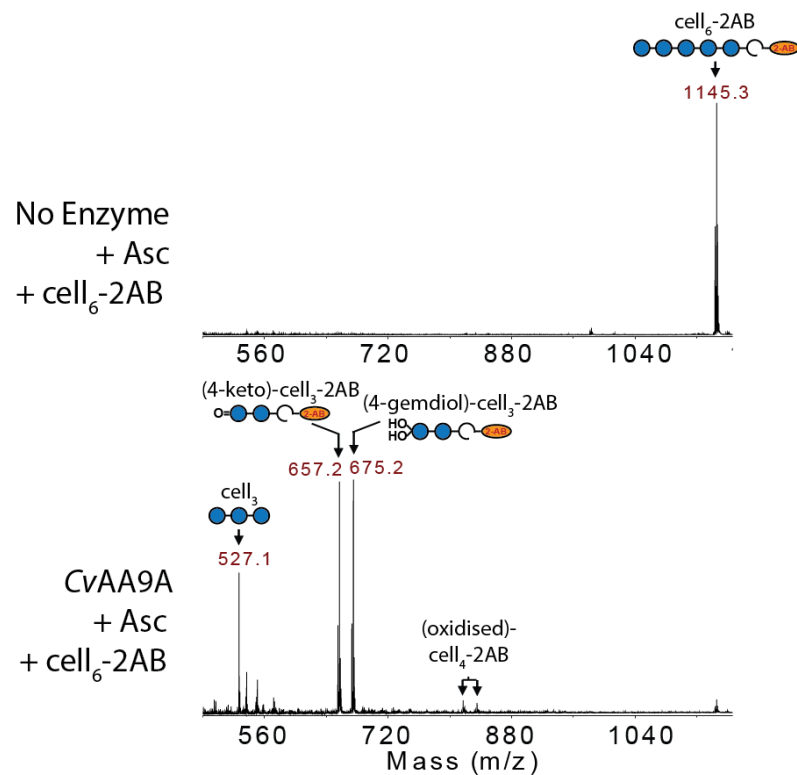
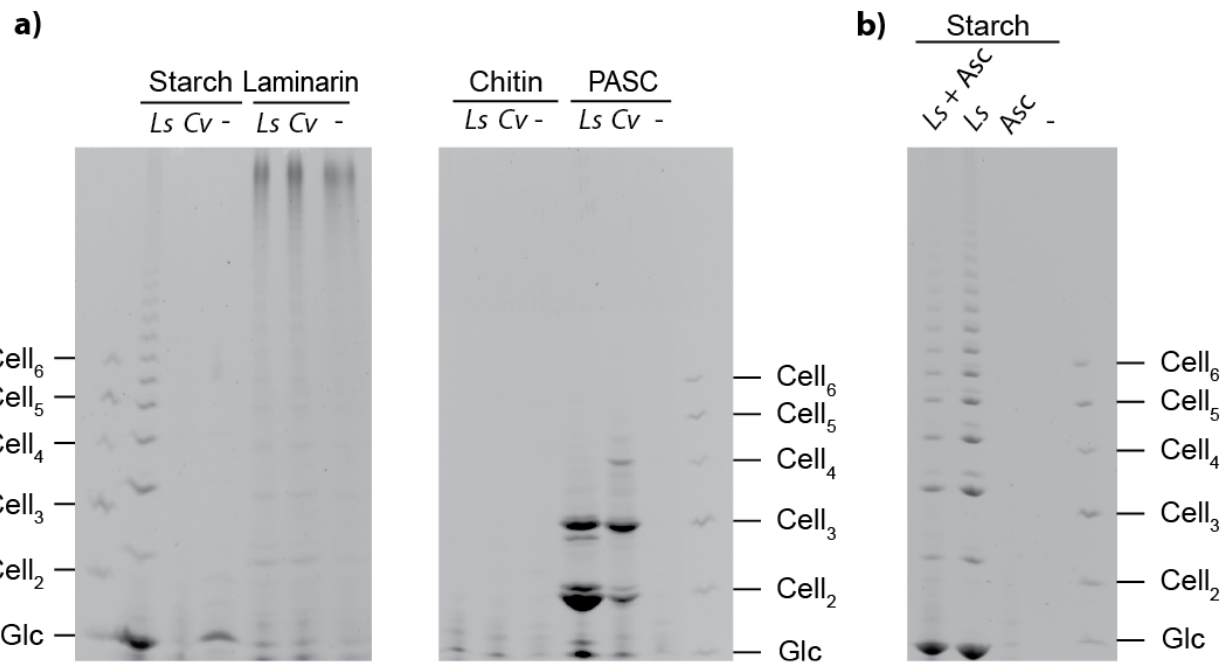


Supplementary Figure 1: Alignment of LsAA9A and CvAA9A enzymes. Copper ligand residues are highlighted in yellow; key residues of LsAA9A involved in protein:substrate interactions are highlighted in green and the equivalent residues of CvAA9A are in purple.

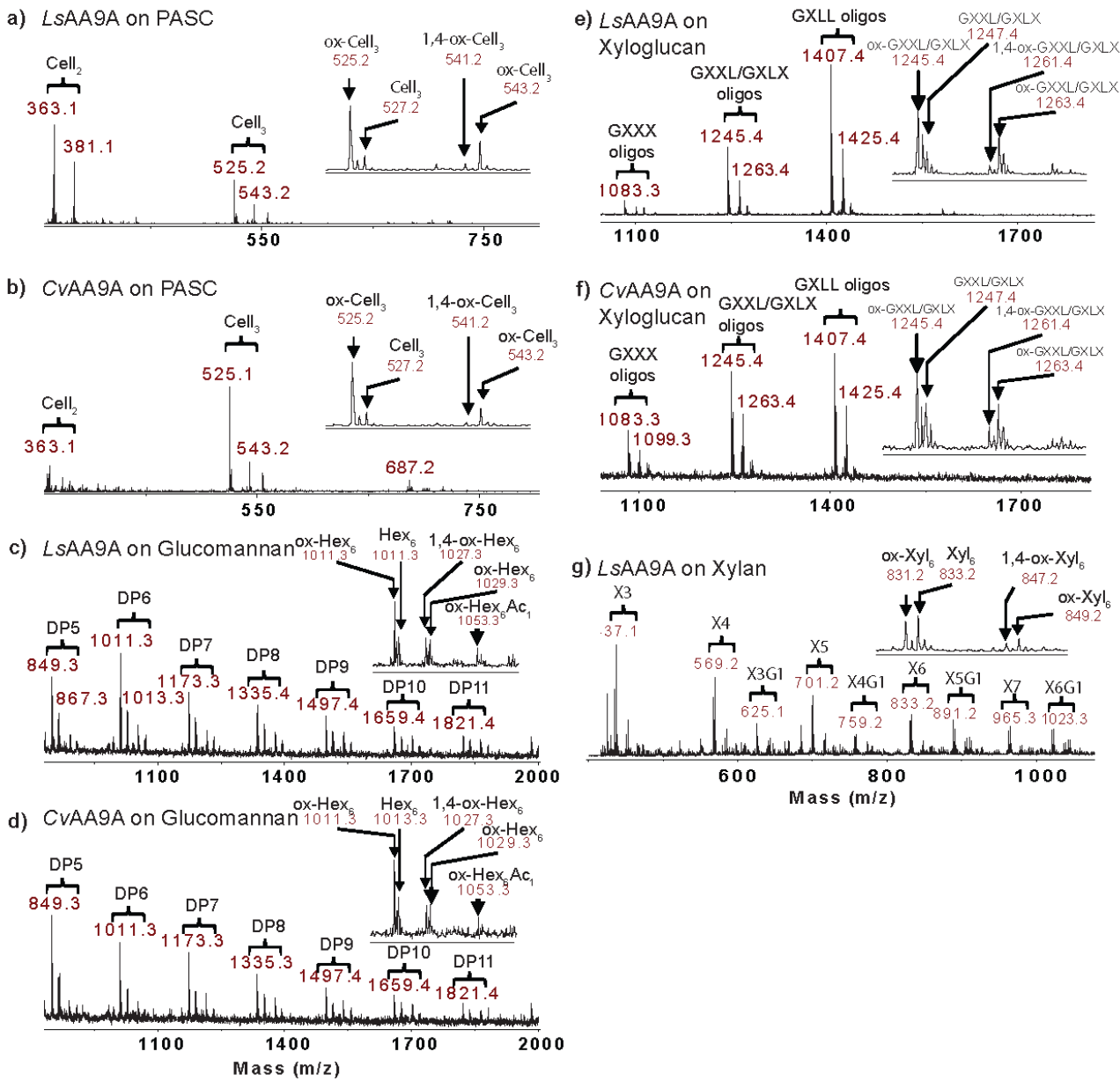


Supplementary Figure 2: CvAA9A cleaves Cell₆-2AB using solely a C4-oxidation mechanism. MALDI-ToF MS spectra showing substrates and products of CvAA9A activity on Cell₆-2AB.

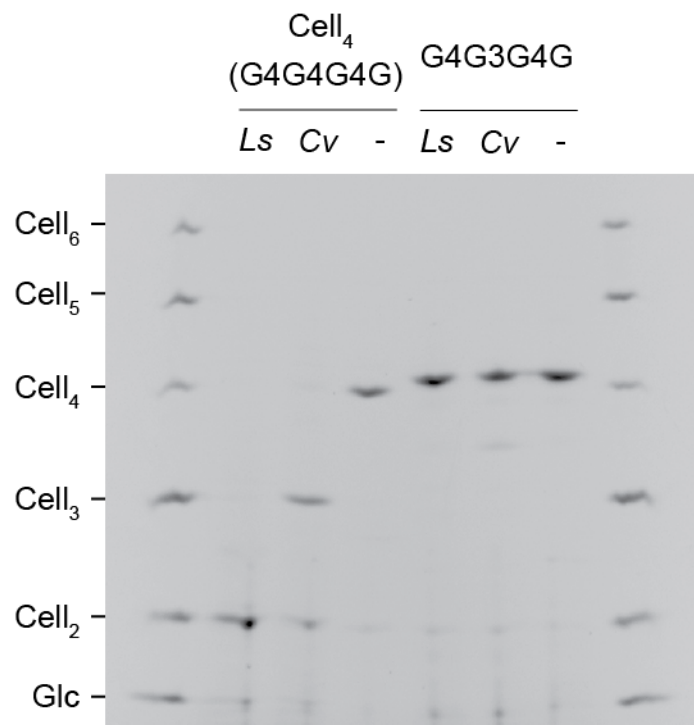


Supplementary Figure 3: *LsAA9A* and *CvAA9A* are unable to cleave a range of polysaccharide structures.

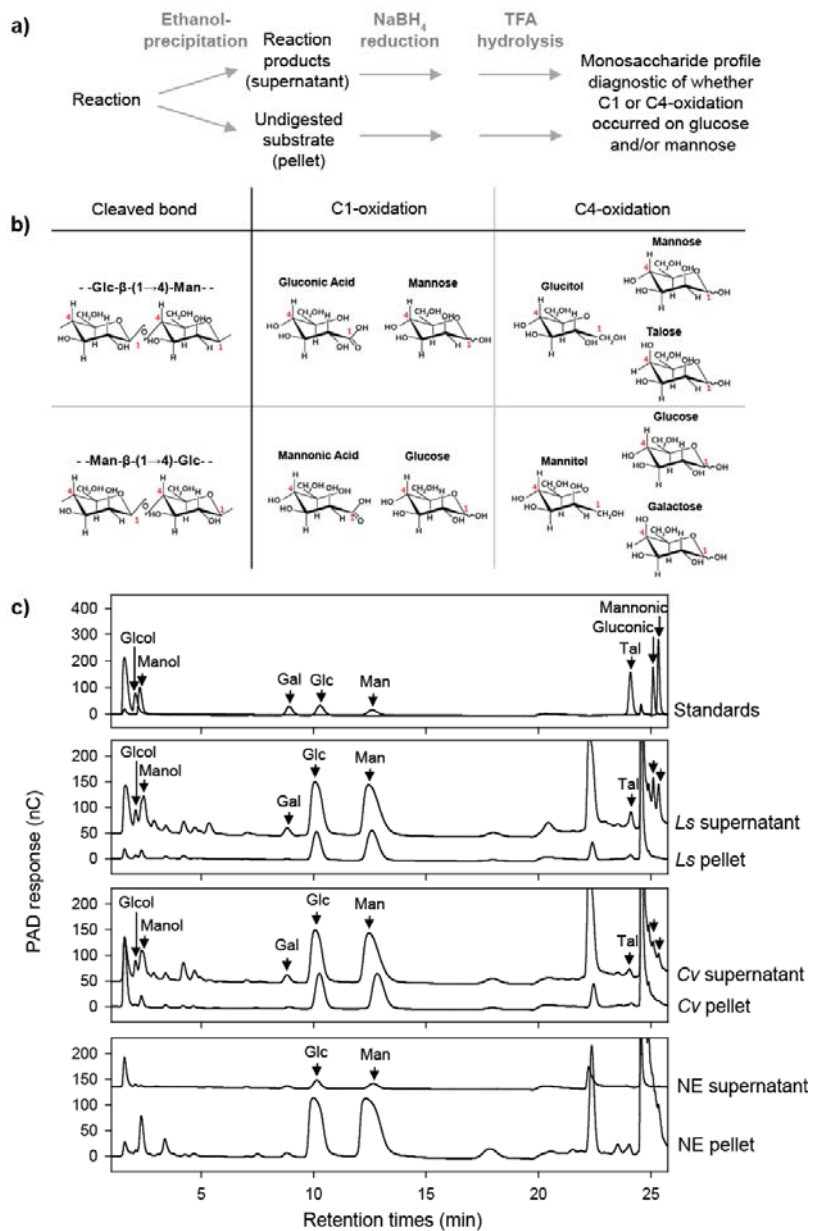
a, PACE gels showing products of *LsAA9A* and *CvAA9A* activity on a range of polysaccharide substrates with 4mM ascorbate. **b**, PACE gel showing products of *LsAA9A* on starch, showing that cleavage by the *LsAA9A* preparation is not reductant-dependent and therefore likely the product of a contaminating hydrolase. *Ls*, *LsAA9A*; *Cv*, *CvAA9A*; *Asc*, ascorbate.



Supplementary Figure 4: MALDI ToF MS spectra of the products of *LsAA9A* and *CvAA9A* on a range of polysaccharide substrates. DP, degree of polymerization; ox-, oxidized oligosaccharides. For xyloglucan nomenclature, see Fry et al¹.

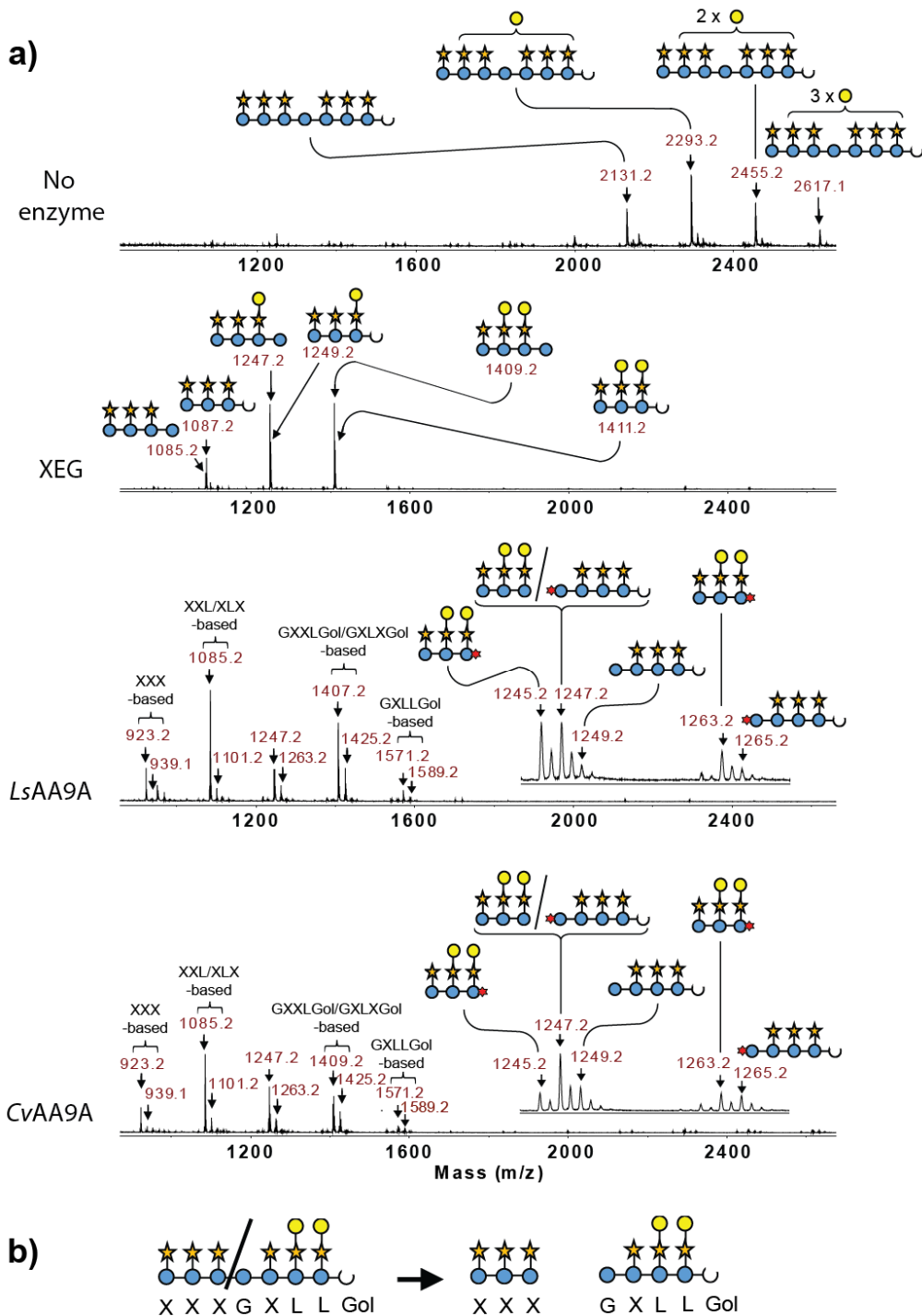


Supplementary Figure 5: *LsAA9A* and *CvAA9A* are able to cleave Cell_4 but not G4G3G4G. PACE gel showing products of *LsAA9A* and *CvAA9A* activity on Cell_4 but not G4G3G4G ($\text{D-Glc-}\beta\text{-}(1\rightarrow 4)\text{-D-Glc-}\beta\text{-}(1\rightarrow 3)\text{-D-Glc-}\beta\text{-}(1\rightarrow 4)\text{-D-Glc}$), with 4mM ascorbate.

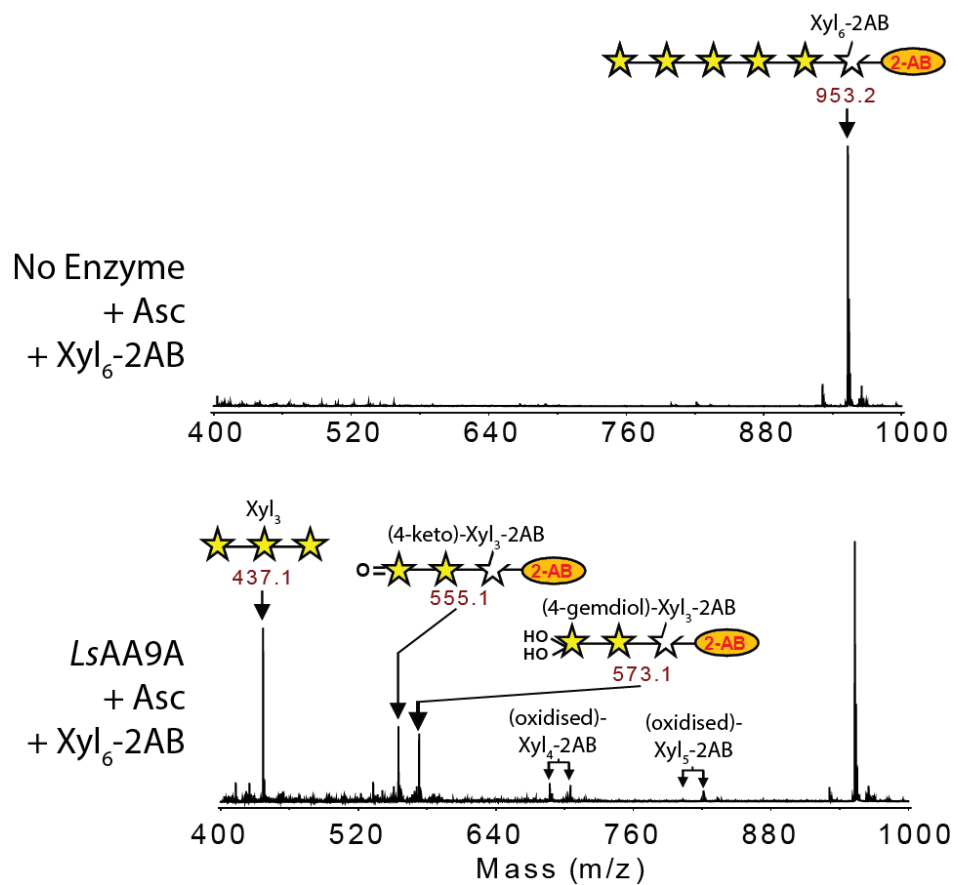


Supplementary Figure 6: LsAA9A and CvAA9A can cleave glucomannan with glucosyl or mannosyl residues at subsites -1 and +1 and yield both C1- and C4-oxidised products

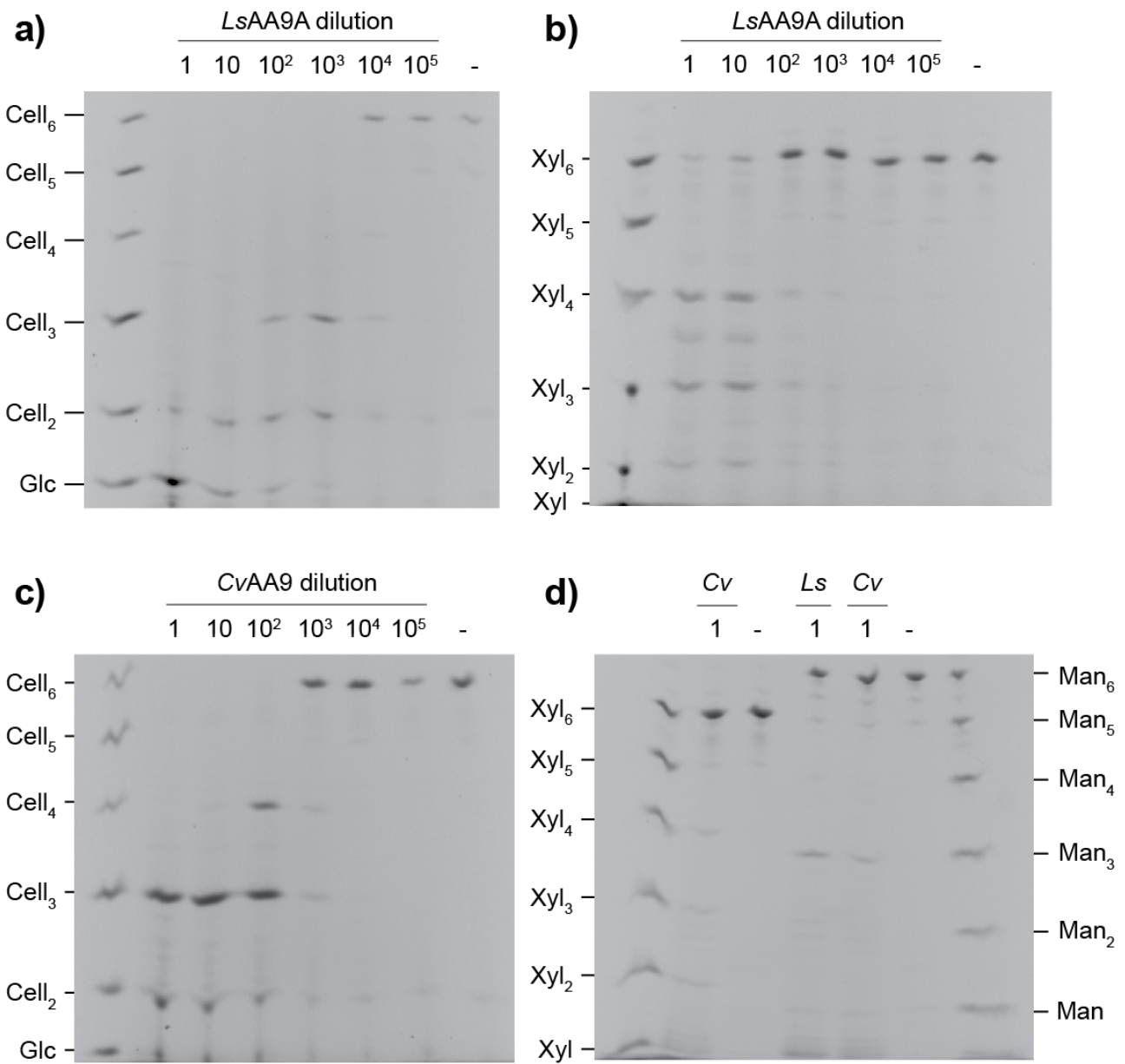
a, Protocol for analysis of site of cleavage and oxidation state **b**, Expected products (following analysis protocol) after C1 or C4 oxidative cleavage of different bonds. **c**, HPAEC analysis of products (supernatant) and undigested substrates (pellet) of LsAA9A and CvAA9A activity on glucomannan. The presence of Talose indicates C4-oxidation of mannose. The presence of mannonic acid indicates C1 oxidation of mannose. All reactions using 4mM ascorbate as reductant. NE, no enzyme. Tal, Talose; Glcol, glucitol; Manol, Mannitol.



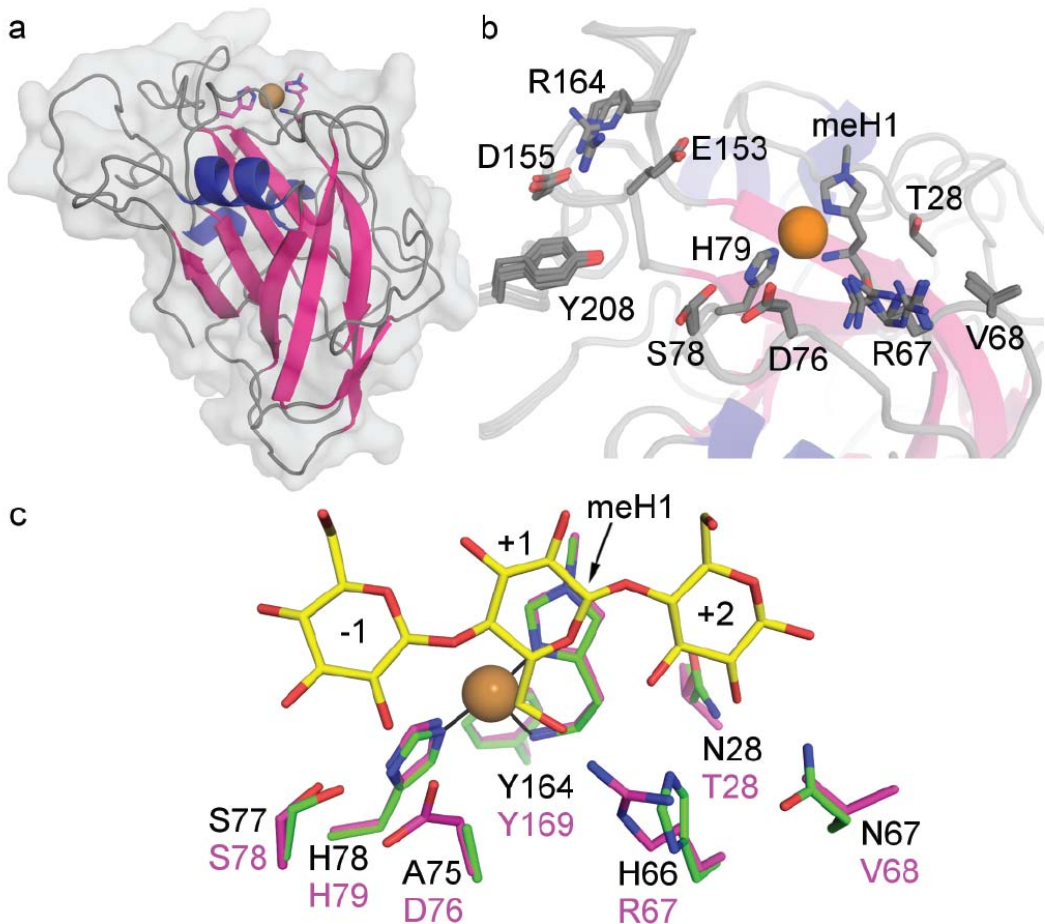
Supplementary Figure 7: *LsAA9A* and *CvAA9A* cleave xyloglucan oligosaccharides with unsubstituted glucose at subsite +1. **a**, MALDI MS spectra showing products of *LsAA9A* and *CvAA9A* activity on a range of di-subunit xyloglucan oligosaccharides. The LPMOs cleave at a different site to xyloglucan endoglucanase (XEG). **b**, Schematic diagram showing cleavage of a xyloglucan oligosaccharide.



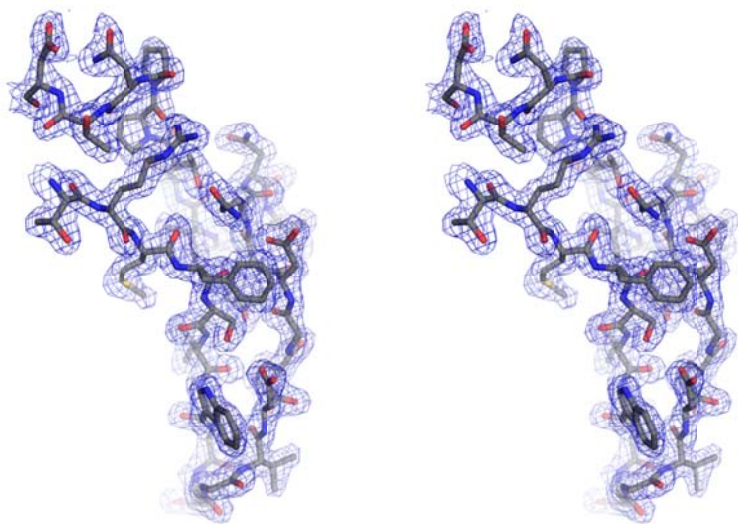
Supplementary Figure 8: *LsAA9A* cleaves Xyl₆-2AB using solely a C4-oxidation mechanism. MALDI MS spectra showing substrates and products of *LsAA9A* activity on Xyl₆-2AB.



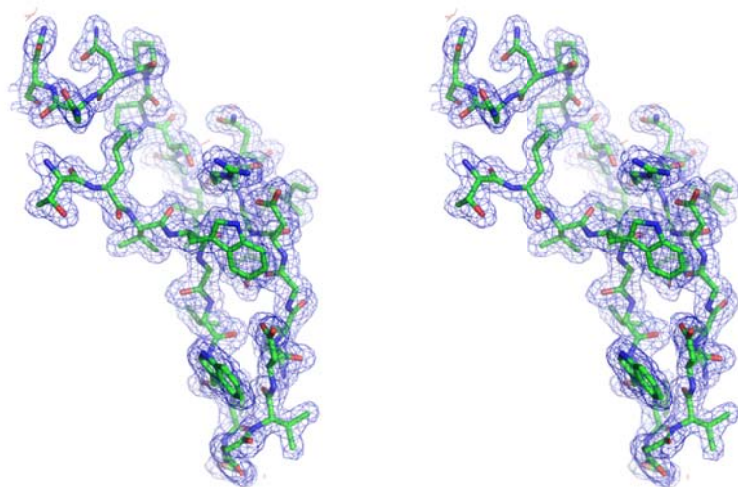
Supplementary Figure 9: *LsAA9A* cleavage of Xyl₆ is much faster than *CvAA9A*. PACE gels showing cleavage of oligosaccharides by different dilutions from standard assay conditions of *LsAA9A* and *CvAA9A* with 4mM ascorbate. a *LsAA9A* on Cell₆, b *LsAA9A* on Xyl₆ c *CvAA9A* on Cell₆ d *CvAA9A* shows no activity of Xyl₆. *LsAA9A* and *CvAA9A* show scarcely detectable activity on Man₆



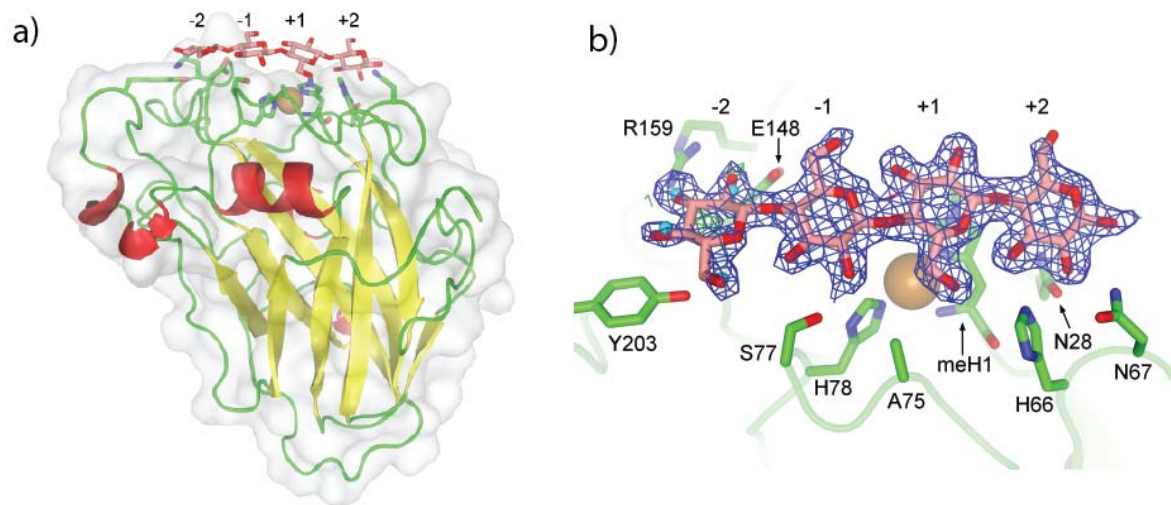
Supplementary Figure 10: CvAA9A structure. **a**, Structure of CvAA9A. **b**, CvAA9A active site. **c**, Structural comparison of residues in *LsAA9A* and CvAA9A. Residues of *LsAA9A* (green, black labels) interacting with Cell₅ (yellow) at subsite -1 to +2 and those equivalent in CvAA9 (chain A - magenta) are shown (part of Cell₅ is not shown for clarity)..



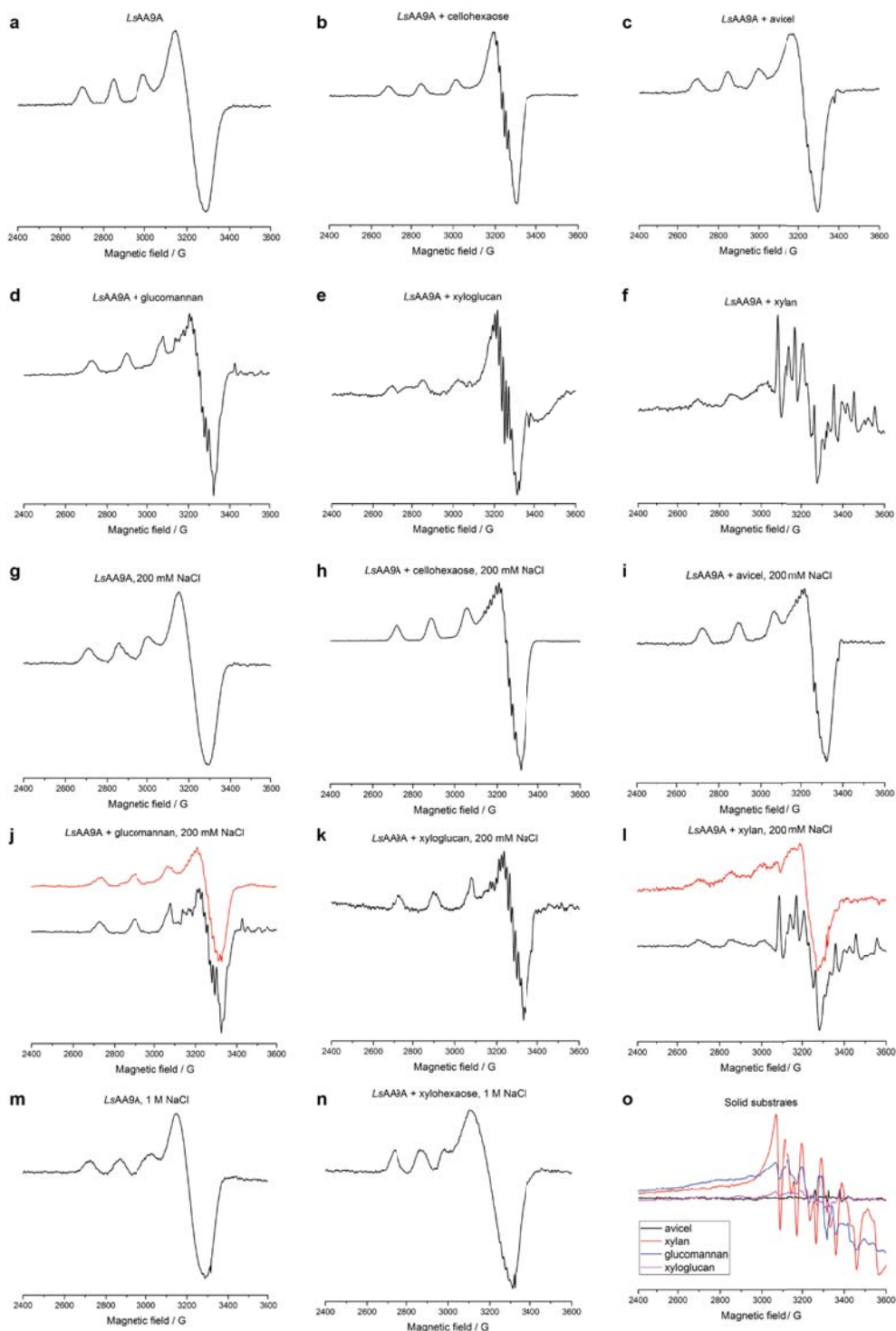
Supplementary Figure 11: Stereo view of representative electron density for the CvAA9A structure determined at 1.90 Å resolution. The region shown covers residues 2-29. The $2F_{\text{obs}} - F_{\text{calc}}$ electron density map is shown contoured at 1σ . Difference electron density is also displayed at $+3\sigma$ (green) and -3σ (red) but is barely visible.



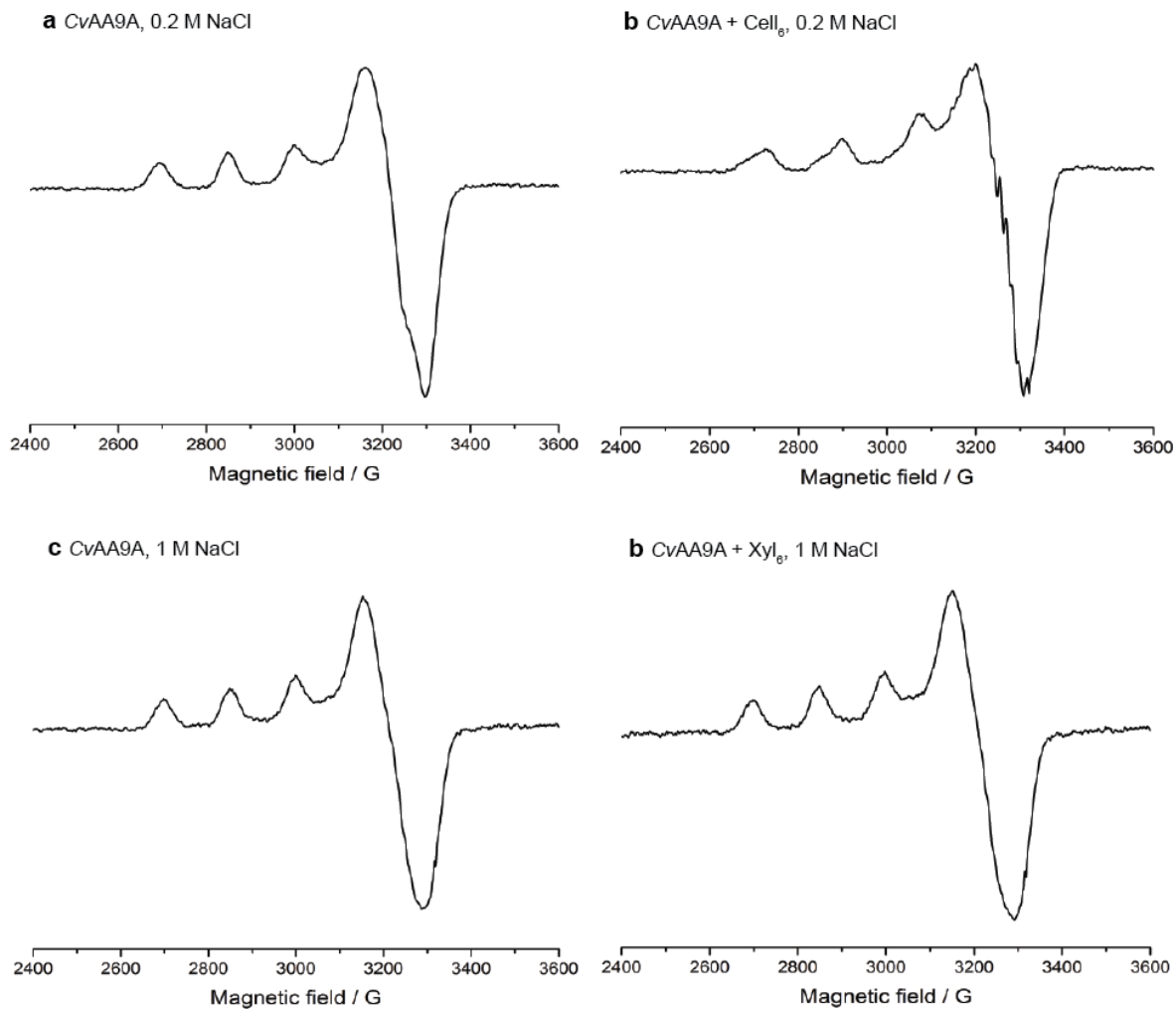
Supplementary Figure 12: Stereo view of representative electron density for the lowest resolution LsAA9A-oligosaccharide complex structure, LsAA9A:G4G4G3G determined at 2.0 Å resolution. The region shown covers residues 2-29. The $2F_{\text{obs}} - F_{\text{calc}}$ electron density map is shown contoured at 1σ . Difference electron density is also displayed at $+3\sigma$ (green) and -3σ (red) but is barely visible.



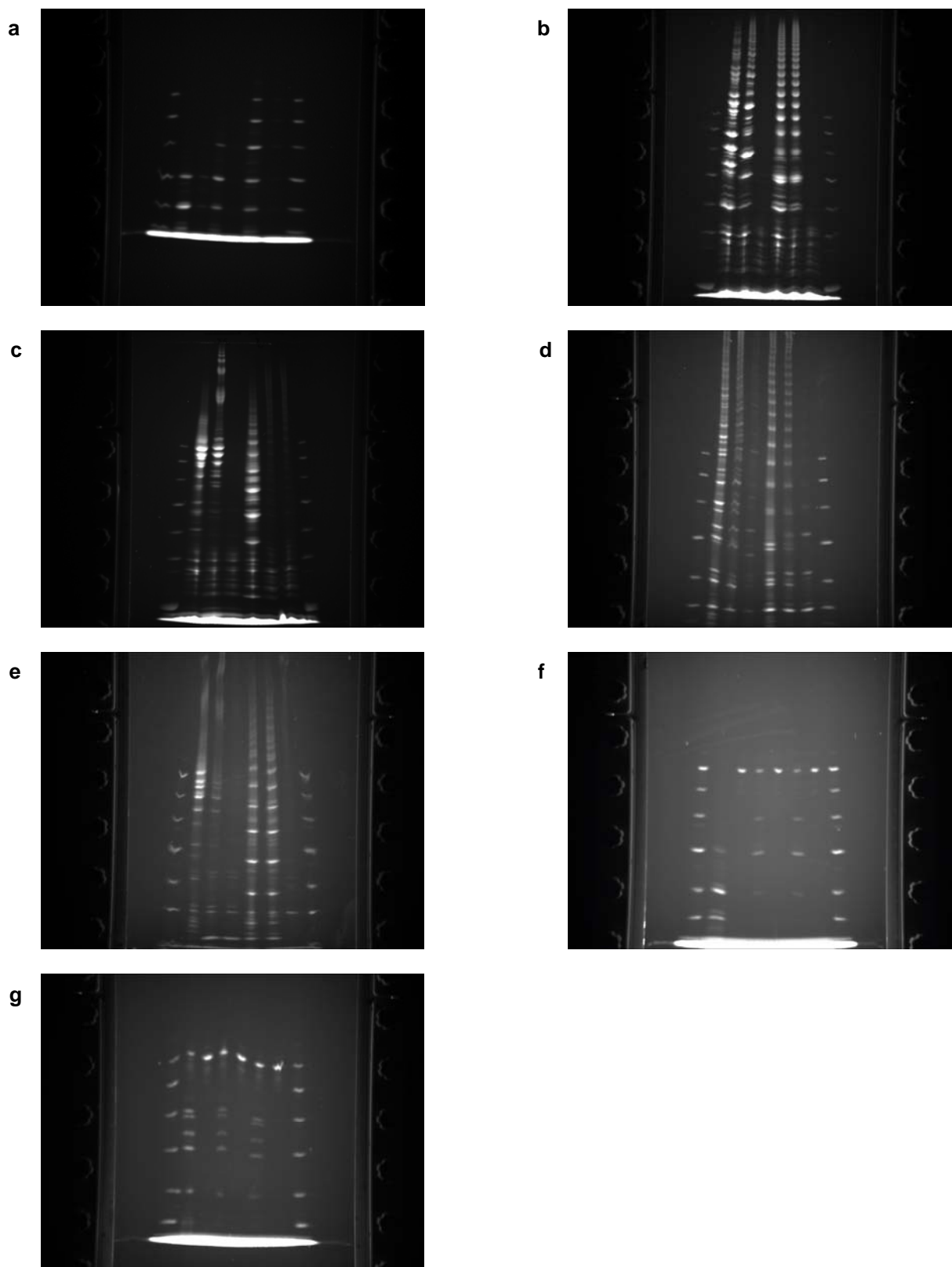
Supplementary Figure 13: Structure of LsAA9A:MLG4. **a**, Structure of *LsAA9A* with MLG4 bound. **b**, zoom-in on active site of *LsAA9A* with MLG4 bound. The $2F_{\text{obs}} - F_{\text{calc}}$ electron density map contoured at 1σ shows β -(1 \rightarrow 4)-glucan density, with no evidence of bound residues with β -(1 \rightarrow 3)-linkages.



Supplementary Figure 14: X-band cw EPR spectra of LsAA9A and various substrates. Spectra a-f were run in chloride-free buffer, spectra g-l in the presence of 200 mM NaCl, spectra m and n with 1 M NaCl. **a.** LsAA9A. **b.** LsAA9A in the presence of 2 equivalents of Cell₆. **c.** LsAA9A with avicel. **d.** LsAA9A and glucomannan. **e.** LsAA9A and xyloglucan. **f.** LsAA9A and xylan. **g.** LsAA9A. **h.** LsAA9A in the presence of 2 equivalents of Cell₆. **i.** LsAA9A with avicel. **j.** LsAA9A and glucomannan or solubilized glucomannan (red). **k.** LsAA9A and xyloglucan. **l.** LsAA9A and xylan or solubilized xylan (red). **m.** LsAA9A. **n.** LsAA9A in the presence of ~150 equivalents of Xyl₆. **o.** solid substrates.



Supplementary Figure 15: X-band cw EPR spectra of CvAA9A. Spectra **a** and **b** run in the presence of 200 mM NaCl, spectra **c** and **d** with 1 M NaCl. **a.** CvAA9A. **b.** CvAA9A in the presence of 4 equivalents of Cell_6 . **c.** CvAA9A. **d.** CvAA9A in the presence of \sim 150 equivalents of Xyl_6



Supplementary Figure 16: Uncropped PACE gels. a. PACE gel from Fig. 1a. **b,c.** PACE gels from Fig. 2a. **d,e.** PACE gels from Fig. 4a. **f,g.** PACE gels from Fig. 4b.

Supplementary Table 1: Accession numbers of characterized LPMOs in the phylogenetic tree of Figure 1.

Label	Accession
GH61-1	EAA30263.1
GH61-2	EAA29018.1
LsAA9A	ALN96977.1
MtLPMO9A	AKO82493.1
MYCTH_112089	AEO60271.1
MYCTH_92668	AEO56665.1
NcLPMO9C	EAA36362.1
NcLPMO9D	CAD21296.1
NcLPMO9E	EAA26873.1
NcLPMO9F	CAD70347.1
NcLPMO9M	EAA33178.1
NCU00836	EAA34466.1
PaLPMO9A	CAP73254.1
PaLPMO9E	CAP67740.1
PaLPMO9H	CAP61476.1
PaLPMO9D	BAL43430.1
PaLPMO9A	ACS05720.1

Supplementary Table 2: glycosidic torsion angles

Glycosidic torsion angles		LsAA9A:Cell ₅	LsAA9A:G4G4G 3G	LsAA9A-Cu(II) :Xyl ₅	LsAA9A:Xyl ₅	LsAA9A:Xyl ₄	LsAA9A:Xyl ₃	LsAA9A:GM
Subsite +2/+3 (°)	Φ	-	-	-	-	-	-	-83.5/-76.7 §
	Ψ	-	-	-	-	-	-	100.9/114.4 §
Subsite +1/+2 (°)	Φ	-89.4	-92.6	-79.7	-75.5	-	-83.6	-93.7
	Ψ	91.7	93.3	-175.6	-175.4	-	140.7	94.9
Subsite -1/+1 (°)	Φ	-83.9	-85.1	-75.1	-80.2	-	(-103.6)* (164.7)*	-82.7 103.3
	Ψ	99.9	96.2	152.5	162.4	-		
Subsite -2/-1 (°)	Φ	-79.0	-66.9	-84.4	-86.3	-86.3	-87.2	-73.4
	Ψ	98.5	94.2	123.1	118.7	107.2	99.4	94.8
Subsite -3/-2 (°)	Φ	-68.7	-	-98.1	-97.7	-113.3	-129.2	-113.7
	Ψ	101.0	-	127.0	130.2	132.3	152.4	126.7
Subsite -4/-3 (°)	Φ	-	-	-	-	-	-	-92.6/-91.2 §
	Ψ	-	-	-	-	-	-	106.1/105.3 §
Ideal cellulose torsion angles	Φ			-88.9				
	Ψ			95.0				
Definitions	Φ			O _{5'} – C _{1'} – O ₄ – C ₄				
	Ψ			C _{1'} – O ₄ – C ₄ – C ₃				
Ideal xylan torsion angles	Φ			-				
	Ψ			-				
Definitions	Φ			O _{5'} – C _{1'} – O ₄ – C ₄				
	Ψ			C _{1'} – O ₄ – C ₄ – C ₃				

§ Alternative conformation
*(xylosyl unit flipped out of subsite-1)

Supplementary Table 3: Protein-substrate interactions.

Potential hydrogen bonding distances (within 3.2 Å distance) in LsAA9A-complex structures												LsAA9A:GM				
		LsAA9A:Cell ₆			LsAA9A:G4G3G			LsAA9A-Cu(II):Xyl ₆			LsAA9A:Xyl ₆			LsAA9A:GM		
Subsite	Glycosidic/	Residue (atom)	Distances (Å)	Residue (atom)	Distances (Å)	Residue (atom)	Distances (Å)	Residue (atom)	Distances (Å)	Residue (atom)	Distances (Å)	Residue (atom)	Distances (Å)	Residue (atom)	Distances (Å)	
+3	O(6)	-	-	-	-	n/a	n/a	n/a	n/a	n/a	n/a	n/a	n/a	H ₂ O	2.70§	
+2	O(1)	H ₂ O	2.30	H ₂ O	3.06	Asn28(Nδ ₂)	2.94	Asn28(Nδ ₂)	2.97	Asn28(Nδ ₂)	3.06	Asn28(Nδ ₂)	2.95	-	-	
	O(1)	-	(Asn67(Nδ ₂))	-	-	Asn67(Oε ₁)	-	Asn67(Nδ ₂)	2.67	Asn67(Nδ ₂)	2.71	Asn67(Nδ ₂)	2.62	Asn28(Nδ ₂)	2.89	
	O(2)	Asn28(Nδ ₂)	2.81	Asn28(Nδ ₂)	2.87	-	-	-	-	-	-	-	-	Asn67(Nδ ₂)	2.67	
	O(2)	Asn67(Nδ ₂)	2.58	Asn67(Nδ ₁)	2.57	-	-	-	-	-	-	-	-	His66(Nε ₂)	2.81	
	O(3)	His66(Nε ₂)	2.80	His66(Nε ₂)	2.72	-	-	-	-	-	-	-	-	-	-	
	O(4)	-	-	-	-	-	-	-	-	-	-	-	-	-	-	
	O(4)	-	-	-	-	His66(Nε ₂)	-	-	-	-	-	-	-	-	-	
	O(5)	-	-	-	-	His66(Nε ₂)	2.80	His66(Nε ₂)	2.76	His66(Nε ₂)	2.76	His66(Nε ₂)	2.75	-	-	
+1	O(6)	H ₂ O _{-pocket}	2.80	H ₂ O _{-pocket}	2.71	n/a	n/a	n/a	n/a	n/a	n/a	n/a	n/a	H ₂ O _{-pocket}	2.83	
-1	O(2)	Ser77(OY)	2.54	Ser77(OY)	2.59	Ser77(OY)	2.65	Ser77(OY)	2.63	Ser77(OY)	2.68	Ser77(OY)	2.57	Ser77(OY)	2.67	
	O(2)	-	-	-	-	-	-	-	-	-	-	*{Gln162((Nδ ₂))}	*{3.16}	-	-	
	O(3)	-	-	-	-	-	-	-	-	-	-	*{Glu148((Oε ₂))}	*{2.60}	-	-	
	O(3)	-	-	-	-	H ₂ O	2.94	H ₂ O	2.95	-	-	*{Ile158((CO))}	*{3.04}	-	-	
	O(4)	-	-	-	-	(Ty203(OH))	-	(Ty203(OH))	-	-	-	*{Ile158((CO))}	*{2.87}	-	-	
	O(6)	-	-	H ₂ O	3.12	n/a	n/a	n/a	n/a	n/a	n/a	n/a	n/a	-	-	
-2	O(2)	Glu148(Oε ₁)	2.58	Glu148(Oε ₁)	2.62	Glu148(Oε ₁)	2.62	Glu148(Oε ₁)	2.66	Glu148(Oε ₁)	2.71	Glu148(Oε ₁)	2.74	Glu148(Oε ₁)	2.55	
	O(2)	-	-	-	-	Arg159(Nω ₁)	2.90	Arg159(Nω ₁)	2.98	Arg159(Nω ₁)	2.90	Arg159(Nω ₁)	2.94	-	-	
	O(3)	Arg159(Nω ₂)	3.02	Arg159(Nω ₂)	3.12	Arg159(Nω ₂)	2.83	Arg159(Nω ₂)	2.93	Arg159(Nω ₂)	2.87	Arg159(Nω ₂)	2.82	Arg159(Nω ₁)	3.13	
	O(3)	-	-	-	-	#Leu222(CO)	3.01	-	#Leu222(CO)	2.82	#Leu222(CO)	2.80	#Leu222(CO)	2.80	H ₂ O	3.04
	O(5)	-	-	-	-	H ₂ O	2.80	H ₂ O	2.67	-	-	-	-	(Asp150(Oδ ₂))	-	
	O(6)	-	-	-	-	(Ty203(OH))	n/a	(Ty203(OH))	n/a	n/a	n/a	n/a	n/a	#Gly233(N)	2.71	
-3	O(5)	-	-	-	-	H ₂ O	2.86	-	-	-	-	-	-	-	-	
	O(6)	Arg159(Nω ₂)	3.01	-	n/a	n/a	n/a	-	n/a	n/a	n/a	n/a	n/a	n/a	-	
	O(6)	Asp150(Oδ ₂)	2.71	-	n/a	n/a	n/a	n/a	n/a	n/a	n/a	n/a	n/a	n/a	-	
	O(6)	#Leu222(CO)	2.60	-	n/a	n/a	n/a	n/a	n/a	n/a	n/a	n/a	n/a	n/a	-	
	O(2)	-	-	-	-	-	-	-	-	-	-	-	-	Asn201(Nδ ₂)	3.13	
	O(2)	-	-	-	-	-	-	-	-	-	-	-	-	Asn201(Nδ ₂)	3.12 §	
	O(3)	-	-	-	-	-	-	-	-	-	-	#Ser219(CO)	2.99	#Ser219(CO)	3.07 §	
	O(3)	-	-	-	-	-	-	-	-	-	-	-	-	#Ser219(CO)	3.07 §	

§ Alternative conformation; * (xy)osy/ unit flipped out of subsite-1; # Symmetry related interaction; n/a not applicable

Supplementary Table 4: Crystallization and soaking conditions

Crystallization Conditions	<i>LsAA9A:Cell₅</i>	<i>LsAA9A:G4G4G3G</i>	<i>LsAA9A:Xyl₃</i>	<i>LsAA9A:Xyl₄</i>	<i>LsAA9A:Xyl₅</i>	<i>LsAA9A:Xyl₅ Cu(II)</i>	<i>LsAA9A:GM</i>	<i>CvAA9</i>
Protein concentration	19.2 mg/mL	19.2 mg/mL	19.2 mg/mL	19.2 mg/mL	19.2 mg/mL	19.2 mg/mL	19.2 mg/mL	6.3 mg/mL
Preincubation [Cu(II)acetate] Time	1.0 mM 1 hour	1.4 mM 30 min	1.0 mM 1 hour	1.0 mM 1 hour	1.0 mM 1 hour			
Precipitant concentration	3.2 M NaCl	3.5 M NaCl	4.4 M NaCl	4.1 M NaCl	3.6 M NaCl	3.6 M NaCl	3.3 M NaCl	1.6 M (NH ₄) ₂ SO ₄ 0.1M NaCl
Reservoir buffer	0.1 M citric acid pH3.5	0.1 M citric acid pH3.5	0.1 M citric acid pH4.5	0.1 M citric acid pH4.0	0.1 M citric acid pH4.5	0.1 M citric acid pH4.5	0.1 M citric acid pH3.5	0.1 M HEPES pH 7.5
drop volume and ratio (Prot:Res:H ₂ O)	0.5 µL 3:1:1	0.4 µL 3:1:0	0.4 µL 3:1:0	0.5 µL 3:1:1	0.4 µL 3:1:0	0.4 µL 3:1:0	0.4 µL 3:1:0	0.5 µL 3:1:1
Soaking Conditions	<i>LsAA9A:Cell₅</i>	<i>LsAA9A:G4G4G3G</i>	<i>LsAA9A:Xyl₃</i>	<i>LsAA9A:Xyl₄</i>	<i>LsAA9A:Xyl₅</i>	<i>LsAA9A:Xyl₅ Cu(II)</i>	<i>LsAA9A:GM</i>	<i>CvAA9</i>
pH equilibration	30 min. in 0.4ul drop of pH 5.5	-	-	-	-	-	-	-
Soaking Conditions	1ul G5 solution added for 10 min	0.5ul of 0.3M MLG-B (reservoir) added for 20 min	1.45 M X3 pH5.5 1 hour	1.25 M X4 pH5.51 hour	0.9M X5 pH 5.5 10 min	0.9M X5 pH 5.5 10 min	GM solution pH 5.5 15 min	-

Both proteins were buffered in 20 mM acetate pH 5.5

Supplementary Reference

1. Fry, S.C. et al. An unambiguous nomenclature for xyloglucan-derived oligosaccharides *Physiol. Plant.* **89**, (1993)